CHARACTERISTICS OF RAIN INFILTRATION IN SOIL LAYERS ON THE HILLSLOPE BEHIND IMPORTANT CULTURAL ASSET

Yuuki Arimitsu[1], Masamitsu Fujimoto[2], Nobutaka Hiraoka[3], Toru Danjo[4], Yuko Ishida[5]
and Ryoichi Fukagawa[6]

[1]Graduate School of Science and Engineering, Ritsumeikan University, Japan,
[2,6] College of Science and Engineering, Ritsumeikan University, Japan,
[3] Research Organization of Science and Technology, Ritsumeikan University, Japan,
[4] Department of Storm Flood and landslide Research, National Research Institute for Earth Science and Disaster Prevention, Japan,
[5]Institute of Disaster Mitigation for Urban Cultural Heritage, Ritsumeikan University, Japan

ABSTRACT: Recently, slope failures have occurred due an increase of heavy rainfall and typhoon events. As typical examples, sediment disasters have occurred frequently at Kiyomizu-dera Temple, including debris flows in 1972 and shallow slope failures in 1999 and 2013. Kiyomizu-dera temple is a UNESCO World Heritage Site, and one of the Historic Monuments of Ancient Kyoto, Japan. An increase in shear stress and decrease in shear strength due to infiltration of rainwater led to slope failures. In this study, subsurface water movements were investigated by measuring pore water pressure changes and hydraulic gradients during rainfall events to prevent damage to important cultural assets by natural disasters. Saturation was found to occur after very small rainfall events, regardless of soil moisture conditions. Although subsurface water normally flows from upper to lower areas of the slope, water movements from the bedrock to the soil layer were observed during rainfall events, suggesting the existence of potentially hazardous slope failure conditions.

Keywords: Slope Failure, Pore Water Pressure, Hydraulic Gradient, Infiltration of Rain Water

1. INTRODUCTION

Recently, slope failures have occurred due to an increase in heavy rainfall and typhoon events in Japan, which cause significant damage. Kiyomizu-dera Temple is located on the slope of a mountain in Higashiyama, Kyoto Prefecture, Japan and was designated a cultural asset of national importance in 1994. Five million tourists from all over the world visit Kiyomizu-dera Temple each year [1]. Sediment disasters have occurred on a number of occasions at Kiyomizu-dera Temple, including a debris-flow event in 1972 and shallow slope failures in 1999 and 2013 [1]. Photo 1 shows a slope failure at Kiyomizu-dera Temple in 2013. It is necessary to forecast landslide and debris flow hazards, to prevent and alleviate damage to an important cultural asset and protect human life.
Previous research has noted that slope failure due to rainfall is triggered by two main factors following rainwater infiltration into the soil. Firstly, an increase in shear stress occurs due to an increase in soil weight. Secondly, a decrease in shear strength occurs due to decreasing soil cohesion. It is therefore necessary to evaluate soil moisture content, soil water movement and groundwater in the soil layer during rainfall events. In-situ measurements of pore water pressures were conducted in a catchment with granitic geology [2], [3] and sedimentary rock geology [4]. These

studies showed that subsurface water movements are more complex in sedimentary rock compared to granitic sites, due to the heterogeneity of the soil structure. The complex responses of pore water pressures in soil on a slope based on sedimentary rock in Kiyomizu-dera Temple have been studied [5]–[7]. However, the subsurface water movements in the soil layer are not fully understood. In this study, subsurface water movements are evaluated by investigating pore water pressure changes and hydraulic gradients during rainfall events.

Photo.1 Slope failure that occurred in 2013

2. METHOD

The study area is located on the hillslope behind Kiyomizu-dera Temple (Fig. 1). The soil-bedrock and measured were composed of sandstone, shale and chert. Surface layer composed of the colluvial deposit ranges 0.9 from to 4.0 m thick. A network system with data loggers was installed (Campbell, CR-1000) to record pore water pressures in real-time. Pore water pressures and rainfall were measured at 10-min intervals, using a tensiometer and tipping-bucket rain gage, respectively. Tensiometers were installed at 14 locations (Fig. 1).

Fig.1 Locations of observation points

Table 1 Observation depths of tensiometers

Points	Observation depths (cm)
A	40, 80, 100
B	40, 80, 100, 200, 260
C	40, 80, 100, 230
D	40, 80, 100
M	20, 40, 60, 80, 100, 190
P1	30, 65
P2	30, 60, 100, 200
P3	30, 80
P4	30, 60, 100
P5	30, 60, 100, 200
P6	30, 60, 100, 200, 280
P7	30, 60, 100
P8	30, 60, 100, 200
P9	30, 60, 110

Table 1 shows the observation depths of the tensiometers. Tensiometer depths were decided based on the results of portable dynamic cone penetration tests. The observation period was from 13 August 2014 to 1 January 2015. Soil depth was measured using a nuclear density cone penetrometer with a weight of 5 kg and fall distance of 50 cm. Nd is the number of blow required to penetrate 2 cm, and we considered Nd > 50 to indicate the soil-bedrock interface. Figure 2 shows the results of cone penetration test at points B, M, P2 and C. The soil depth at points B, M, P2 and C were 2.65 m, 1.95 m, 2.04 m and 2.29 m, respectively.

3. RESURTS AND DISCUSSION

3.1 Characteristic of Pore Water Pressures

Pore water pressures at points B, M, P2 and C (yellow points on Fig. 1) were evaluated to investigate subsurface water movements along the longitudinal direction of the slope. Figure 3 shows the variation of pore water pressure during the observation period (13 August 2014 to 1 January 2015). The cumulative rainfall during the period was 634 mm, with a peak rainfall of 38 mm/h at 13:00 on 16 August 2014. Pore water pressures reached positive values at each observation depth, indicating saturation at these depths. Decreases in
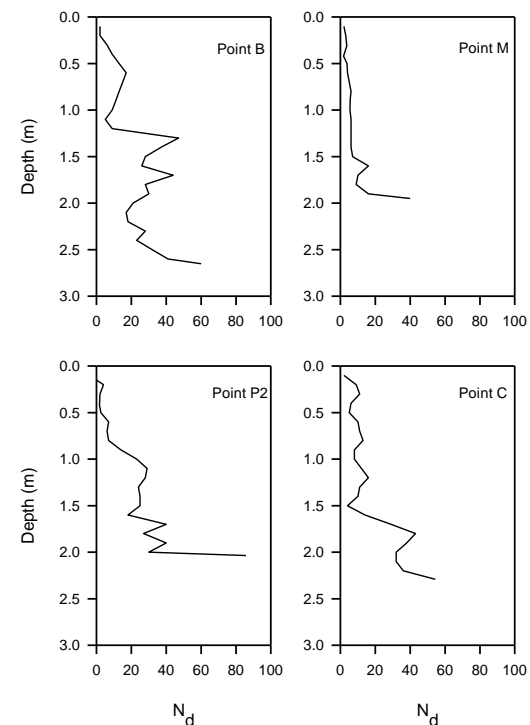

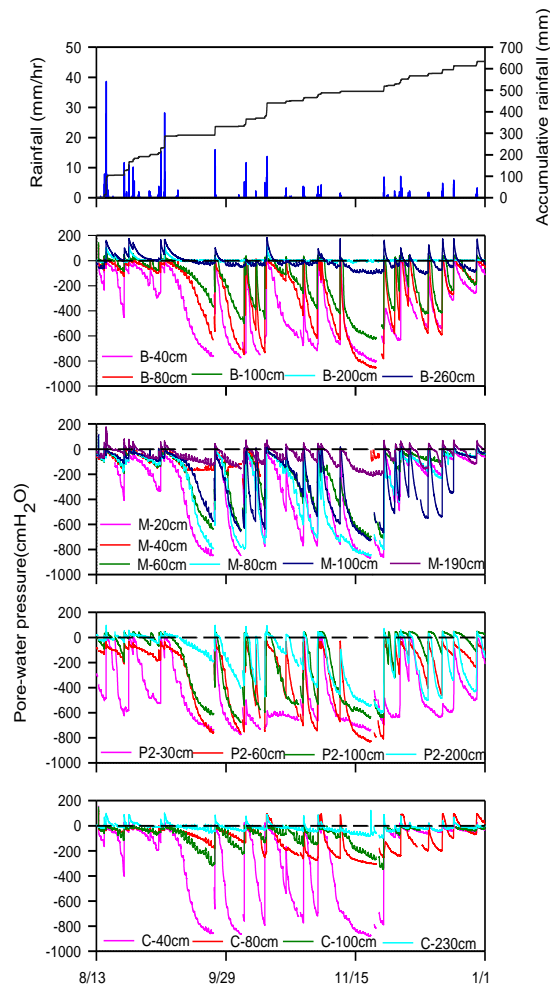Fig.2 N_d value profiles in soil at points B, M, P2 and C

Fig.3 Variation in the pore water pressure during rainfall events

pore water pressures after rainfall at deep observation depths (B-200 cm, B-260 cm M-190 cm and C-230) were smaller than those at shallow observation depths, indicating that deep soils retained wet conditions over a long period of time. However, at sampling points P2-200 cm (the soil-bedrock interface), pore water pressures varied widely compared to other points at the soil-bedrock interface (B-260 cm, M-190 cm and C-230 cm). These results indicate that changes in pore water pressure showed different trends according to observation point and depth.

3.2 Direction of Subsurface Flow

The hydraulic gradient across the study area was investigated to evaluate groundwater flow in the soil layer. Figure 4 shows (a) hyetograph and hydraulic gradient between (b) B-40 cm and B-80 cm, (c) B-80 cm and B-100 cm, (d) B-100 cm and B-200 cm, (e) B-200 cm and B-260 cm. The hydraulic gradient was calculated from the
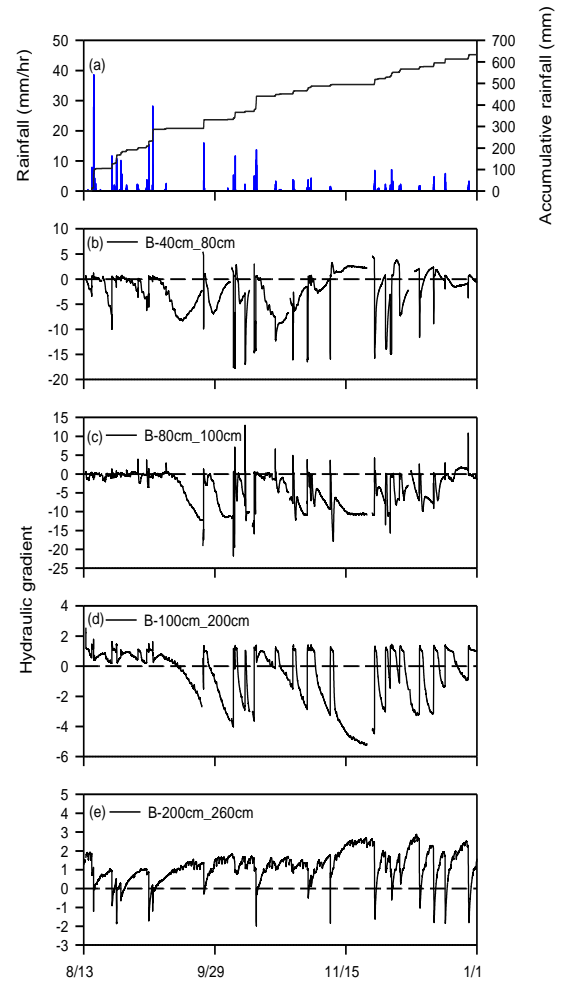

Fig.4 (a) Hyetograph and hydraulic gradient between (b) B-40 cm and B-80 cm, (c) B-80 cm and B-100 cm, (d) B-100 cm and B-200 cm, and (e) B-200 cm and B-260 cm

hydraulic head and the distance between two observation depths. Hydraulic gradients with positive values indicate downward vertical flow between two observation depths at the same measurement point, while hydraulic gradients with negative values indicate upward vertical flow between two observation depths at the same point. The hydraulic gradients had negative values before the start of a rainfall event, and reached positive values during rainfall events (Fig. 4 b, c and d). This result indicates that the direction of soil water movement during dry conditions was from deep to shallow soil layers by evapotranspration and that infiltration occurred after rainfall events. The hydraulic gradients were positive before the start of rainfall and attained negative values during rainfall (Fig.4e). The result at point B indicated water movement from deep to shallow layers during rainfall events. This suggests that
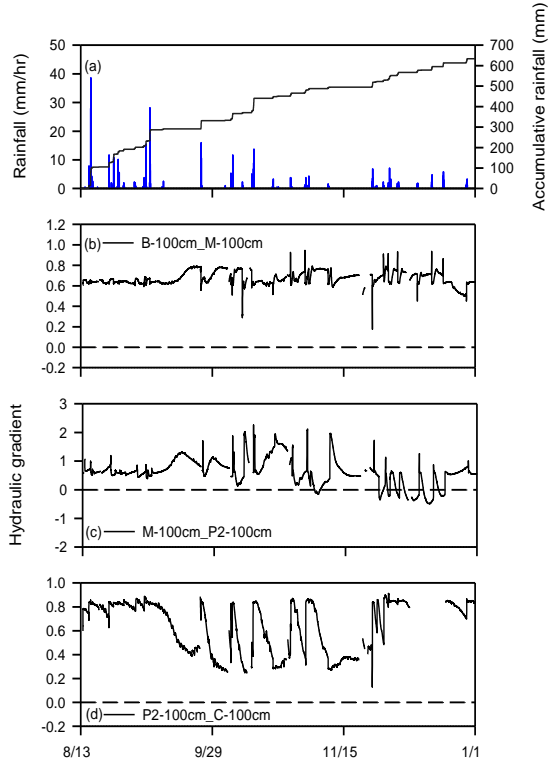
Fig.5 (a) Hyetograph and hydraulic gradient between (b) B-100 cm and M-100 cm, (c) M-100 cm and P2-100 cm, and (d) P2-100 cm and C-100 cm (between each depth of 100 cm)
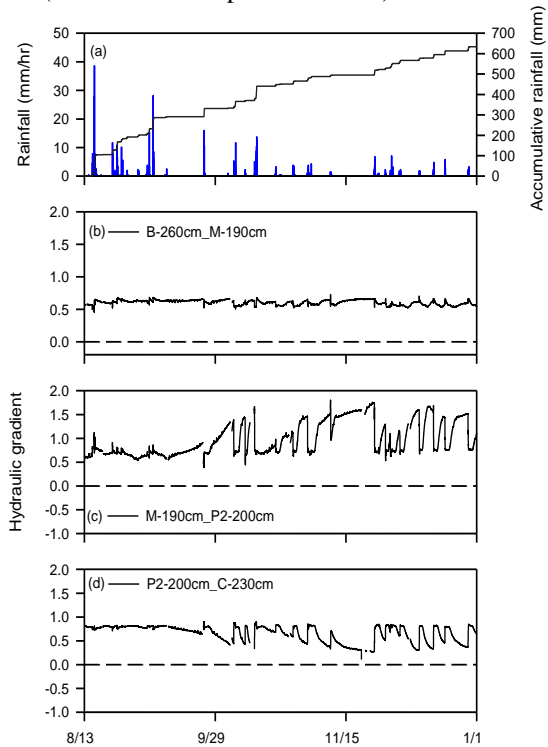

Fig.6 (a) Hyetograph and hydraulic gradient between (b) B-260 cm and M-190 cm, (c) M-190 cm and P2-200 cm, (d) P2-200 cm and C-230 cm
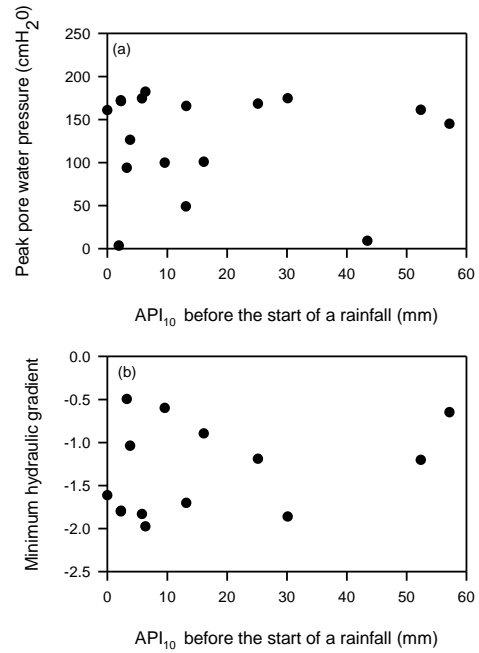

Fig.7 Relationships between the API_{10} before the start of a rainfall and (a) peak pore water pressure at B-260cm, and (b) minimum hydraulic gradient

exfiltration from the bedrock layer to the soil layer occurred at this point, leading to a high probability of slope failure. Figure 5 shows (a) hyetograph and hydraulic gradient between (b) B-100 cm and M-100 cm, (c) M-100 cm and P2-100 cm, (d) P2-100 cm and C-100 cm (between each depth of 100 cm). Hydraulic gradients showed positive values during the observation period, indicating that subsurface water flows from the upper to lower levels of the slope at all times (Fig. 5b and d). Figure 5 c indicates that the hydraulic gradient reached negative values during the period 26 November 2014 to 1 January 2015. In addition, hydraulic gradients at deep observation points were positive during the entire observation period, indicating that subsurface water flows from the upper to lower areas of the slope (Fig. 6).

API_{10} was used to model the residual effect of previous rainfall [3].

$$API = \sum_{i=1}^{10} (P_i / i) \qquad (1)$$

where P is the total amount of rainfall (i days before-hand)

At point B-260 cm, there were no clear relationships between the soil moisture conditions (wet and dry) of the before start of a rainfall and
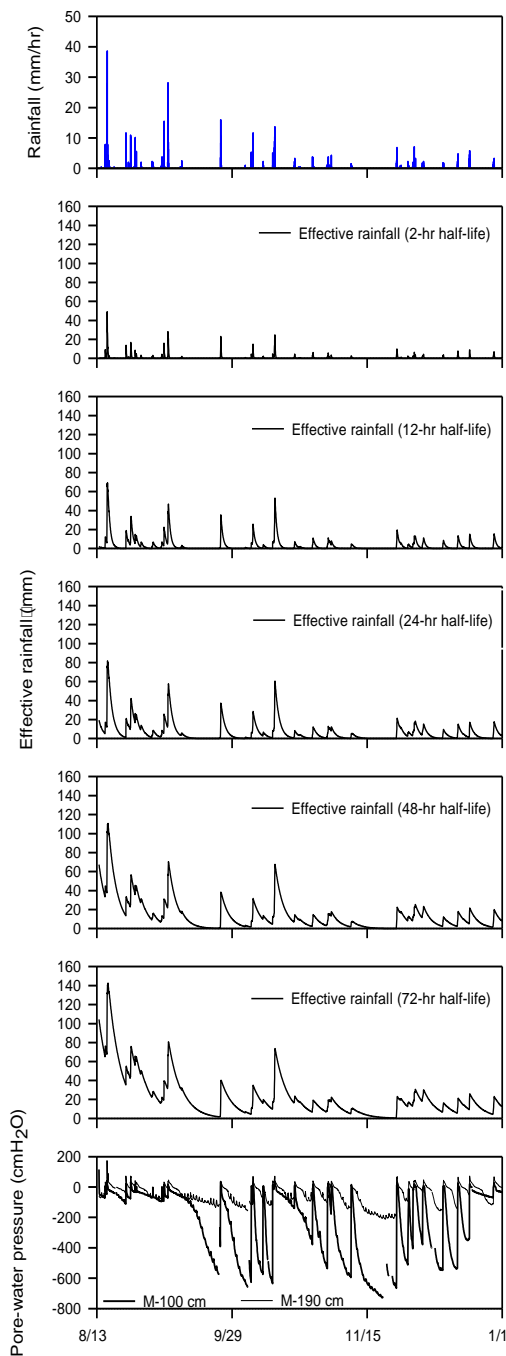
Fig.8 Hyetograph, effective rainfall, and pore water pressure at M-100 cm and M-190 cm during the observation period

peak pore water pressure (Fig.7 a). In addition, when API_{10} of before the start of a rainfall was small, hydraulic gradient reached negative values (Fig.7 b). These results indicated that at point B, for dry conditions of before the start of rainfall, exfiltration from the soil-bedrock layer to the soil layer occurred.
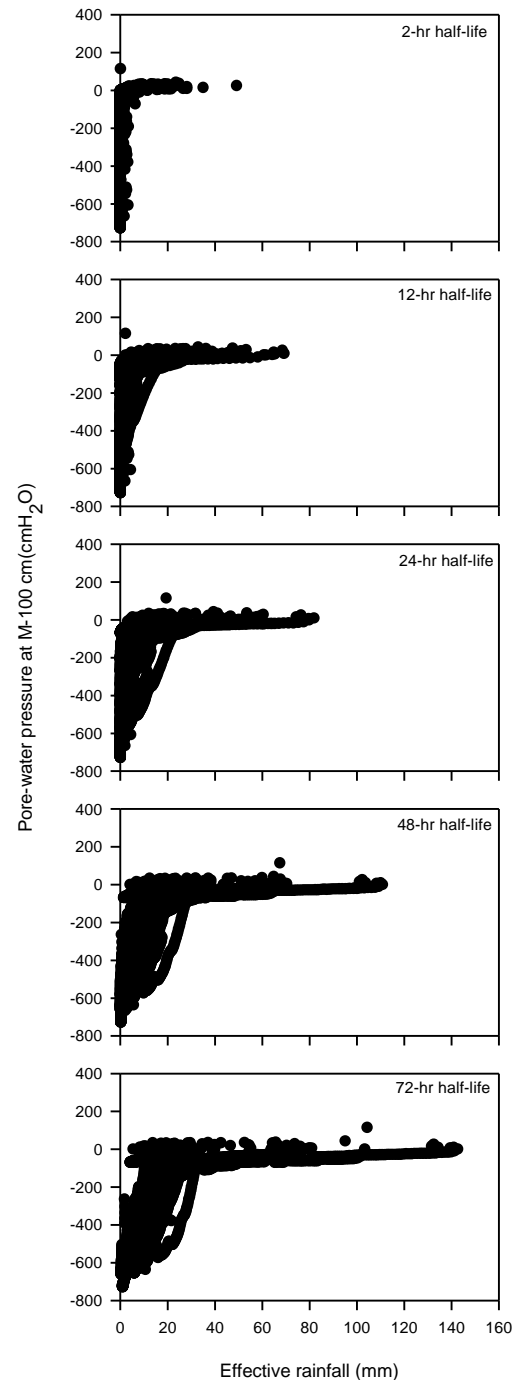

Fig.9 Relationship between the pore water pressure at the M-100-cm point and the effective rainfall

3.3 Effect of Soil Moisture Conditions on Subsurface Flow

To evaluate the relationships between the antecedent rainfall and the pore water pressure response, the effective rainfall was calculated using the method proposed by Suzuki and Kobashi [8].
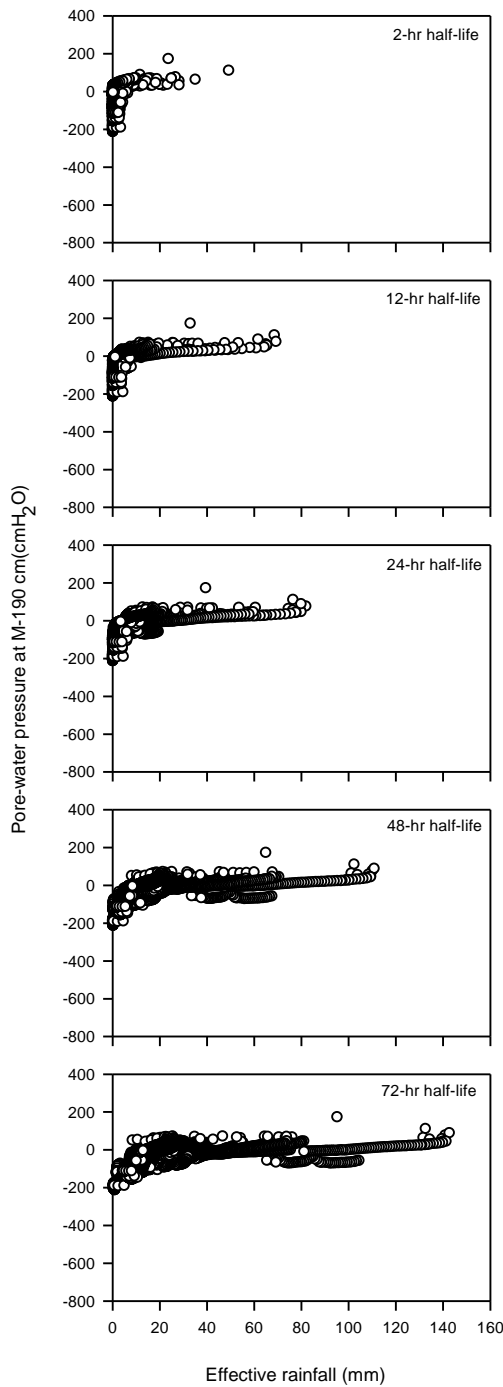
Fig.10 Relationship between the pore water pressure at the M-190-cm point and the effective rainfall

$$M = (\ln 0.5)/\alpha \qquad (2)$$

$$D_M(T) = D_M(T-1)e^{\alpha} + R(T)e^{\alpha/2} \qquad (3)$$

where M is the half-life, α is a reduction factor, D_M is the effective rainfall (mm), T is time (hour) and $R(T)$ is the rainfall (mm/h).
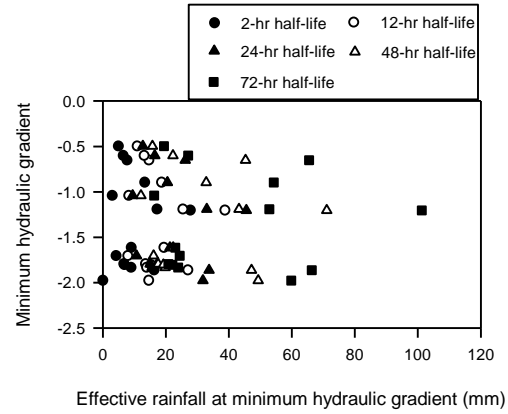

Fig.11 Relationship between the minimum hydraulic gradient (between B-200 cm and B-260 cm) and effective rainfall at minimum hydraulic gradient
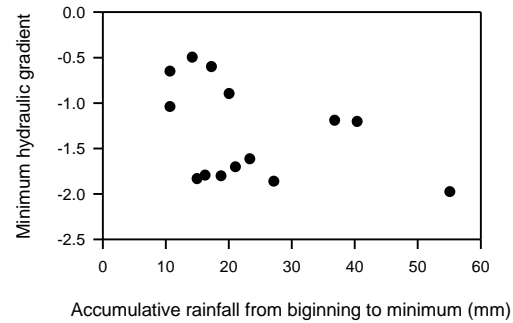

Fig.12 Relationship minimum hydraulic gradient (between B-200cm and B-260 cm) and accumulative rainfall from beginning to minimum

Values of effective rainfall for six half-life cases (2 h, 12 h, 24 h, 48 h, and 72 h) were calculated (Fig.8). In the calculation, we considered the rainfall until 13 August 2014. The peaks of effective rainfall with half-lives of 2 h, 12 h, 24 h, 48 h and 72 h were 49 mm, 69 mm, 81 mm, 110 mm and 142 mm, respectively (Fig. 8). Figures 9 and 10 show the relationship between the pore water pressures at sampling points M-100 cm and M-190 cm, respectively, and the effective rainfall. The negative values of pore water pressures at 100 cm were larger than those at the soil-bedrock interface. At points M-100 cm and M-190 cm, the positive values of pore water pressure were constant throughout the observation period regardless of the difference in effective rainfall. In addition, the results indicate that saturation occurred at small values of effective rainfall. For dry periods, although values of pore water pressure were strongly influenced by the antecedent rainfall (i.e., long half-life), the effects were limited to a short time period after rainfall events.

Here, we focused on observation point of B

(between B-200 cm and B-260cm) because the exfiltration from the soil-bedrock layer to the soil layer occurred. Figure 11 showed relationship between the minimum hydraulic gradient and effective rainfall at minimum hydraulic gradient. The direction of soil water movement was from soil-bedrock to the soil layer even by very small effective rainfall. Figure 12 showed relationship between the minimum hydraulic gradient and accumulative rainfall from beginning to minimum. More than 10mm accumulative rainfall from beginning to minimum, hydraulic gradient reached minimum values. In addition, minimum hydraulic gradient were constant regardless of the amount of accumulative rainfall from beginning to minimum. Therefore, the occurrence of exfiltration processes were not depend on the characteristics of rainfall event.

4. CONCLUSION

In this study, subsurface water movements were evaluated by investigating pore water pressure changes and hydraulic gradients during rainfall events. Decreases in pore water pressures after rainfall at deep observation depths were smaller than those at shallow depths, indicating that deep soil layers retained wet conditions over a long time period. The hydraulic gradient at point B indicated different trends between shallow layers and the soil-bedrock interface. Hydraulic gradients between 100 cm depth and the soil-bedrock interface were positive during the observation period, indicating that subsurface water flowed from the upper area to the lower end of the slope at all times. These results indicate that the saturation occurred after very small amounts of rainfall, regardless of soil moisture conditions. At point B, the direction of soil water movement was from soil-bedrock to the soil layer were recognized even in dry conditions and small rainfall amounts.

5. ACKNOWLEDGEMENTS

6. REFERENCES

[1] Ishida Y, Fujimoto M, Hiraoka N, Oya A, Sako K and Fukagawa R, "Study on criteria for slope failure based on rainfall intensity at Kiyomizu-dera", Journal of Disaster Mitigation for Historical Cities, Vol.8, 2014,

[2] Uchida T, Asano Y, Mizuyama T and McDonnell J, "Role of upslope soil pore pressure on lateral subsurface storm flow dynamics", Water Resources Research, Vol.40, 2004, W12401.

[3] Fujimoto M, Ohte N and Tani M, "Effects of hillslope topography on hydrological responses in a weathered granite mountain, Japan: comparison of the runoff response between the valley-head and the side slope", Hydrological Processes, Vol.22, 2008, pp. 2581-2594.

[4] Onodera S, "Subsurface water flow in the Multi-Layered hillslope", Journal of Geographical Review of Japan, Vol.64A-8, 1991, pp. 549-568 (in Japanese with English abstract).

[5] Sako K, Fukagawa R and Satomi T, "Slope monitoring system at a slope behind an important cultural asset", Journal of Disaster Research, Vol.6, No.1, 2011, pp.70-79.

[6] Fujimoto M, Danjo T, Tsuchiyama T, Kimura T and Fukagawa R, "Detection of ground water movement using measuring method of sound of groundwater flow on the hillslope behind Kiyomizu Temple", Journal of Disaster Mitigation for Historical Cities, Vol.8, 2014, pp.145-150 (in Japanese with English abstract).

[7] Danjo T, Fujimoto M, Kimura T, Hiraoka N and Fukagawa R, "Adamage of the slope around the Kiyomizu temple by the heavy rain from the Typhoon in 2013, and a study of the changing moisture in the ground of the slope behind an important cultural asset", Journal of Disaster Mitigation for Historical Cities, Vol.8, 2014, pp. 115-122 (in Japanese with English abstract).

[8] Suzuki M and Kobashi S, "The critical rainfall for the disasters caused by slope failures", Journal of Erosion Control Engineering, Vol.34, 1981, pp.16-26 (in Japanese with English abstract).

Corresponding Author: Yuuki Arimitsu